Polymer 120 (2017) 119–128

Contents lists available at ScienceDirect

Polymer

journal homepage: www.elsevier.com/locate/polymer

Well-defined single-chain polymer nanoparticles via thiol-Michael addition

A. Pia P. Kröger [a], Roy J.E.A. Boonen [a], Jos M.J. Paulusse [a, b, *]

[a] Department of Biomolecular Nanotechnology, MESA+ Institute for Nanotechnology, Faculty of Science and Technology, University of Twente, P.O. Box 217, 7500 AE Enschede, The Netherlands
[b] Department of Nuclear Medicine and Molecular Imaging, University Medical Center Groningen, P.O. Box 30.001, 9700 RB Groningen, The Netherlands

ARTICLE INFO

Article history:
Received 25 March 2017
Received in revised form
5 May 2017
Accepted 15 May 2017
Available online 16 May 2017

ABSTRACT

A synthetic strategy has been developed giving facile access to well-defined single-chain polymer nanoparticles (SCNPs) from styrene-, acrylate- and methacrylate-based polymers. Random copolymers (polydispersity indices 1.10–1.15) of methyl (meth)acrylate, benzyl methacrylate or styrene containing protected thiol monomers (xanthate and thioacetate vinyl monomers) were obtained via reversible addition–fragmentation chain transfer (RAFT) polymerization. Through aminolysis of the xanthate and thioacetate moieties, copolymers with free thiol moieties were obtained. The thiol bearing polymers were cross-linked with bifunctional acrylates under mild conditions. Precursor polymer dependent size-reductions between 30 and 90% were verified by gel permeation chromatography (GPC) measurements. Furthermore, the SCNPs were characterized by ^{1}H NMR, atomic force microscopy (AFM) and dynamic light scattering (DLS). Characteristic patterns for SCNPs were observed in the AFM phase mode. Thiol-Michael addition is demonstrated to be a versatile tool, which can easily be employed in the preparation of versatile well-defined functional polymer nanoparticles in the 3–10 nm size range.

1. Introduction

Developments in the fields of organic chemistry and polymer chemistry over the last decades have resulted in a plethora of synthetic techniques that can be used to fabricate tailor-made polymeric materials, with a large degree of freedom in structure, composition and functionality [1–3]. The synthesis of polymeric nanoparticles has been extensively developed over the past decade, notably by applying techniques such as solvent evaporation [4], nanoprecipitation [5], salting-out [6], spray-drying [7], controlled cross-linking polymerization [8,9], and emulsion polymerization techniques [10]. Owing to their versatility, polymer nanoparticles have found abundant use in nanotechnology with specific focus on the development of novel biomedical applications, such as imaging [11], gene transfection [12,13], and drug delivery [14,15], as well as therapeutics [16]. Additionally, polymeric nanoparticles are investigated as additives in composite membranes for CO_2 capture [17–19], dye separation [20] and water purification [21]. However, widespread industrial application of polymeric nanoparticles is still pending.

Especially for biomedical application of nanoparticles, particle size is known to be of key importance [22]. Nanoparticles below 10 nm in size are particularly of interest as they are rapidly excreted by the kidney and therefore bypass the urgent need of biodegradability [23–26]. Through rapidly establishing equilibria with the vascular compartment, as well as with the lymphatic vessels, nanoparticles with an effective size comparable to that of proteins (<6 nm) exhibit short clearance times in the body [26]. However, only a limited number of methods is currently available for preparation of polymer nanoparticles smaller than 10 nm. These methods include employing (metallo)surfactants or polymer matrices, which function as template during the preparation [27–30].

An elegant and convenient way of achieving smaller, size-controlled polymeric nanoparticles is to cross-link polymer chains intramolecularly, while simultaneously avoiding intermolecular cross-links, yielding so-called single-chain polymeric nanoparticles (SCNP) [31,32]. Under these conditions, nanoparticle

* Corresponding author. Department of Biomaterials Science and Technology, MIRA Institute for Biomedical Technology and Technical Medicine, Faculty of Science and Technology, University of Twente, P.O. Box 217, 7500 AE Enschede, The Netherlands.
E-mail address: j.m.j.paulusse@utwente.nl (J.M.J. Paulusse).

http://dx.doi.org/10.1016/j.polymer.2017.05.040
0032-3861/

properties, such as molecular weight, dispersity and polarity, are directly related to the polymeric precursor. In this respect, controlled polymerization techniques provide for a straightforward way to produce well-defined polymer precursors and hence well-defined nanoparticles.

The first SCNPs were already described in 1962 by Kuhn and coworkers [33], but their development stagnated due to difficulties with characterization and isolation of the particles, as well as the need for ultra-high dilution conditions and the lack of well-defined precursor polymers [32,34–36]. In 2002, Hawker and coworkers devised a method to avoid the need for special separation techniques and ultra-high dilution conditions by designing benzylcyclobutane functional polymers, which only cross-link at elevated temperatures [37]. Through slow addition of the polymer to a heated solution, the need for dilution is reduced to the time period of the cross-linking event (cyclobutane dimerization), since the resulting product particles can be considered chemically inert. However, the harsh reaction conditions limited the practicality of this approach.

In 2009, the same group further refined the system by designing a 2-component system consisting of an isocyanate functional polymer and a diamine as an external cross-linker [38]. The so-called cross-linker mediated chain-collapse bears the advantage that cross-linking does not occur before the two reactive species are combined [31]. Owing to slow, continuous addition of the reactive polymer to the cross-linker, intramolecular coupling at higher concentrations was achieved at room temperature [38]. Since then, the development of intramolecular coupling techniques, driven by the demand for mild and orthogonal reactions, has undergone tremendous progress [32,37,39]. The reactivity of the components required in the different cross-linking techniques unfortunately restricts the number of functional comonomer species that can be incorporated and, likewise a variety of crosslinking techniques is necessary for broad applicability of SCNPs. The portfolio of alternative cross-linking strategies includes click-chemistry [39], photodimerization [40], olefin and alkyne cross-metathesis [41,42], and even non-covalent interactions [43], such as hydrogen bonding [44,45] and metal coordination [46], providing means to design size-controlled nanoparticles with practically any type of functionality [47]. These techniques have in common that the employed crosslinking reactions are extremely fast, thereby vastly promoting intramolecular cross-link formation. Previously, thiol chemistry was utilized in SCNP formation by thiol-ene, thiol-yne [48] and disulfide exchange reactions [49,50]. Furthermore, classical Michael addition cross-linking was employed in the formation of SCNPs, although the reaction speeds limited its practicability [51,52].

Michael addition of thiols to acrylates is in general a rapid reaction, but Hoyle and Lowe demonstrated that the use of phosphines as catalyst results in an exceedingly fast nucleophile-initiated thiol-Michael addition [53]. Besides serving as a catalyst for thiol-Michael addition, phosphines further act as reducing agent to suppress thiol oxidation. Thiol-Michael addition is referred to as a 'click-reaction' due to its mild reaction conditions, high yields, and its high efficiency and selectivity, all of which make it an ideal technique for polymer modification [54–56]. Employing thiol chemistry on polymers, raises the challenge to incorporate either the acrylate group or the thiol into a defined polymer, both of which interfere with controlled radical polymerizations [57,58]. Thiols in particular can initiate chain transfer fragmentation reactions and lead to undesired side reactions during radical polymerization, but effective approaches to circumvent this via protective group chemistry have been reported [59]. Nicolaÿ et al. investigated the tolerance of thiol protection groups towards controlled polymerization techniques such as reversible addition-fragmentation chain transfer (RAFT), showing that neither xanthate, nor thioacetate moieties initiated chain transfer reactions, hence enabling incorporation of thiols into polymers [60]. Furthermore, the thiols are protected from disulfide formation and can be liberated when required.

In this work, we introduce SCNP formation via thiol-Michael addition as a mild cross-linking technique that can be performed at room temperature and in the presence of water. Xanthate- and thioacetate-functional monomers were prepared (Fig. 1) and incorporated into (meth)acrylate and styrene polymers via RAFT copolymerization. To compare the effects of polymer length, incorporation ratio and monomer type, a range of copolymers was prepared and used in the preparation of SCNPs, which were characterized in detail (Fig. 2).

2. Experimental section

Materials. Potassium ethyl xanthogenate (96%), 2-bromoethanol (95%), potassium thioacetate (98%), thioacetic acid (96%), potassium hydroxide (85%), methacryloyl chloride (98%), acryloyl chloride (97%), methyl methacrylate (99%), methyl acrylate (99%), benzyl methacryate (96%), chlorobenzene (99.9%), 2-cyano-2-propyl benzodithioate (97%), 2,2′-azobis(2-methylpropionitrile) (AIBN, 98%), hydrazine monohydrate (98%), 1,4-butanediol diacrylate (90%), tri(*n*-butyl) phosphine (93.5%), 2-(dimethylaminoethyl) acrylate (DMAEA, 98%), 2-naphthol (99%), styrene (99%) and 4-vinylbenzene chloride (90%) were purchased from Sigma Aldrich. Acetone (100%), dichloromethane (100%), ethyl acetate (99.9%), methanol (100%), *n*-heptane (99.8%) and tetrahydrofuran (THF, 100%) were purchased from VWR. Triethyl amine (≥99%) was purchased from Fisher and chloroform (≥99%) was purchased from Merck. All chemicals were used without further purification unless stated otherwise. 2-(Butylthiocarbonothioylthio)propionic acid was prepared following a literature procedure [61]. 4-Vinylbenzyl chloride, methyl methacrylate and benzyl methacrylate were filtered over neutral alumina prior to usage to remove inhibitors. 4-Vinylbenzyl thioacetate was synthesized following a literature procedure [62] and stored with hydroquinone at 4 °C. When stated as dry, solvents were treated with molecular sieves (4 Å) 24 h before usage.

^{1}H NMR (400 MHz) and ^{13}C NMR spectra were recorded on a Bruker 400 spectrometer. Chemical shifts are reported in ppm and referenced to chloroform. Gel permeation chromatography (GPC) was performed on a Waters e2695 Separations Module equipped with an Agilent PLgel 5 μm MIXED-D 300 × 7.5 mm column and Waters photodiode array detector (PDA 2998), fluorescence detector (FLR 2475) and refractive index detector (RI 2414). Chloroform was employed as eluent and molecular weights were

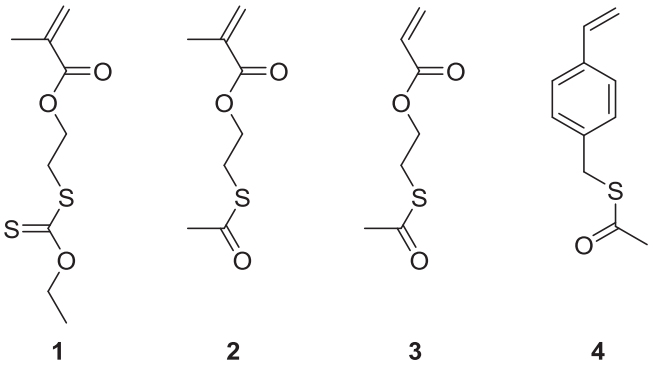

Fig. 1. Employed vinyl monomers with protected thiol moieties.

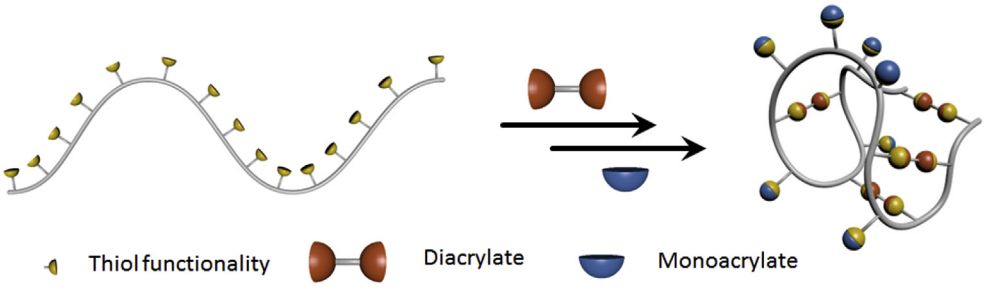

Fig. 2. Schematic representation of polymer chain collapse via thiol-Michael addition.

calibrated relative to linear polystyrene. Dynamic Light Scattering (DLS) measurements were carried out in chloroform on a Malvern Instruments Zetasizer ZS. Samples for DLS and GPC were prepared in chloroform, followed by filtration using GE Healthcare Whatman SPARTAN 13/0.2 RC 0.2 μm syringe filters.

Atomic force microscopy (AFM) images were recorded using a custom-built atomic force microscope. For processing of AFM images, Scanning Probe Image Processor software (version 2.3206) by Image Metrology ApS was used in conjunction with Gwyddion software (version 2.41) by the Czech Metrology Institute. AFM images were plane corrected using line-wise leveling with a third-degree least mean squares fit.

For AFM sample preparation, a 1 mg/mL solution of the product in chloroform was filtered using a GE Healthcare Whatman SPARTAN 13/0.2 RC 0.2 μm syringe filter and diluted with chloroform to 10^{-10} mg/mL. After each step of the serial dilution, the solution was sonicated for 5 min. Immediately after the last sonication, 20–25 μL samples were drop-casted on freshly cleaved mica.

Scanning transmission electron microscopy (STEM) images were recorded on a Zeiss Merlin HR-SEM with an add-on STEM detection system. 5 μL of the sample at a concentration of 10^{-4} mg/mL in chloroform were drop-casted on formvar coated copper grids and incubated for 60 s. Subsequently, the excess of the solution was removed via filter paper. For staining, the grid was incubated for 20 s with 5 μL of a 1% (w/v) uranyl acetate solution.

Monomer synthesis. 2-(Ethyl xanthate) ethyl methacrylate (**1**) was prepared via a 2-step synthesis following earlier reports [63]. 4-Vinylbenzyl thioacetate (**4**) was synthesized according to a modified literature procedure [62].

Synthesis of *S*-2-hydroxyethyl-*O*-ethyldithiocarbonate. A 250 mL round bottom flask was charged with potassium ethyl xanthogenate (20.0 g, 125 mmol) in acetone (75 mL). Under continuous stirring, a solution of 2-bromoethanol (17.2 g, 137 mmol, 1.1 eq.) in acetone (50 mL) was added dropwise over 5 min to the solution. The mixture was stirred at room temperature overnight. Solids were removed via filtration and washed with acetone. The filtrate was concentrated under reduced pressure and dissolved in chloroform (200 mL). Subsequently, the solution was washed with brine (3 × 100 mL). The organic fractions were combined and dried over $MgSO_4$ and solvent was removed under reduced pressure. Excess 2-bromoethanol was removed by dissolving the liquid in toluene (2 × 50 mL), followed by evaporation under reduced pressure, yielding a yellow liquid (14.0 g, 68% yield). ^{1}H NMR (400 MHz, $CDCl_3$) δ_H: 4.59 (q, 2H), 3.79 (t, 2H), 3.28 (t, 2H), 3.02 (1H, OH), 1.37 (t, 3H). ^{13}C NMR (100 MHz, $CDCl_3$) δ_C: 214.4, 70.4, 60.5, 38.2, 13.7.

Synthesis of 2-(ethyl xanthate) ethyl methacrylate (1). A solution of *S*-2-hydroxyethyl-*O*-ethyl dithiocarbonate (14.9 g, 90 mmol) and triethylamine (16 mL, 116 mmol, 1.3 eq.) in dry dichloromethane (100 mL) was cooled down in an icebath. A solution of methacryloyl chloride (10.8 mL, 112 mmol, 1.2 eq) in dry dichloromethane (40 mL) was added dropwise to the stirred solution, resulting in the mixture turning red. After addition was complete, the reaction mixture was left to stir at room temperature overnight. Water (10 mL) was added to neutralize any remaining methacryloyl chloride. The mixture was washed consecutively with water (2 × 150 mL), aqueous hydrochloric acid (2 × 150 mL, 0.5 M), sodium hydroxide solution (2 × 150 mL, 0.5 M) and brine (1 × 150 mL). The combined organic phases were dried over $MgSO_4$ and concentrated under reduced pressure. Following silica column chromatography (*n*-heptane and ethyl acetate (90:10) as eluent) an almost odorless, pale yellow liquid was obtained (17.9 g, 85% yield). ^{1}H NMR (400 MHz, $CDCl_3$) δ_H: 6.13 (m, 1H), 5.59 (m, 1H), 4.66 (q, 2H), 4.39 (t, 2H), 3.45 (t, 2H), 1.95 (m, 3H), 1.43 (t, 3H). ^{13}C NMR (100 MHz, $CDCl_3$) δ_C: 213.8, 167.2, 136.1, 126.2, 70.5, 62.3, 34.5, 18.4, 13.9.

Synthesis of S-(2-hydroxyethyl) ester. A 250 mL round bottom flask was charged with potassium thioacetate (11.4 g, 100 mmol) in acetone (100 mL). Under continuous stirring, a solution of 2-bromoethanol (13.8 g, 110 mmol, 1.1 eq.) in acetone (40 mL) was added dropwise over 5 min to the solution. The mixture was stirred at room temperature overnight and solids were removed via filtration and subsequently washed with acetone. The filtrate was concentrated under reduced pressure and dissolved in chloroform (150 mL). Subsequently, the solution was washed with brine (3 × 100 mL). The organic fractions were combined and dried over $MgSO_4$ and solvent was removed under reduced pressure as washed with brine (3 × 100 mL). Excess 2-bromoethanol was removed by dissolving the liquid in toluene (2 × 50 mL), followed by evaporation under reduced pressure, yielding a yellow liquid (10.0 g, 83% yield).

^{1}H NMR (400 MHz, $CDCl_3$) δ_H: 3.76 (t, 2H), 3.08 (t, 2H), 2.36 (s, 3H). ^{13}C NMR (100 MHz, $CDCl_3$) δ_C: 196.3, 61.3, 31.8, 30.5.

v**Synthesis of 2-(acetylthio) ethyl methacrylate (2).** A solution of methacryloyl chloride (8.5 mL, 81 mmol, 1.3 eq) in dry dichloromethane (30 mL) was added dropwise over 5 min under stirring to an ice-cold solution of *S*-2-hydroxyethyl-thioacetate (7.5 g, 62 mmol) and triethylamine (11.0 mL, 81 mmol, 1.3 eq) in dry dichloromethane (75 mL). The mixture was stirred for 1 h in an ice-bath and was left stirring at room temperature overnight. Water (6 mL) was added to neutralize any remaining methacryloyl chloride. The mixture was washed with water (2 × 150 mL) and aqueous hydrochloric acid (2 × 150 mL, 0.5 M). The organic phases were combined and dried over $MgSO_4$ and concentrated under reduced pressure. Following silica column chromatography (*n*-heptane and ethyl acetate (90:10) as eluent) an almost odorless, pale yellow liquid was obtained (17.9 g, 85% yield).

^{1}H NMR (400 MHz, CDCl3) δ_H: 6.11 (s, 1H), 5.58 (m, 1H), 4.24 (m, 2H), 3.18 (t, 2H), 2.35 (s, 3H), 1.93 (s, 3H). ^{13}C NMR (100 MHz, $CDCl_3$) δ_C: 194.9, 167.0, 136.0, 126.0, 63.0, 30.5, 27.9, 18.3.

Synthesis of 2-(acetylthio) ethyl acrylate (3). A solution of acryloyl chloride (8.7 mL, 108 mmol, 1.3 eq) in dry dichloromethane (50 mL) was added drop wise over 5 min under stirring to an ice-cold solution of *S*-2-hydroxyethyl-thioacetate (10.0 g, 83 mmol) and triethylamine (11.5 mL, 83 mmol, 1.0 eq) in dichloromethane (150 mL). The mixture was stirred for 1 h in an ice-bath and was left stirring at room temperature overnight. Water (10 mL) was added to neutralize any remaining acryloyl chloride. The mixture was washed with water (3 × 250 mL) and aqueous hydrochloric acid (3 × 250 mL, 0.5 M). The organic phases were combined and dried over $MgSO_4$ and concentrated under reduced pressure. Following silica column chromatography (*n*-heptane and ethyl acetate (90:10) as eluent) an almost odorless, clear liquid was obtained (3.30 g, 23% yield).

^{1}H NMR (400 MHz, CDCl3) δ_H: 6.41 (dd, 1H), 6.11 ppm (dd, 1H), 5.85 (dd, 1H), 4.26 (t, 2H), 3.18 (t, 2H), 2.35 (s, 3H). ^{13}C NMR (100 MHz, $CDCl_3$) δ_C: 195.0, 165.9, 131.4, 128.2, 63.0, 30.7, 28.0.

Synthesis of S-(4-vinylbenzyl) thioacetate (4). In a 250 mL 3-necked round bottom flask, equipped with a condenser, potassium hydroxide (8.50 g, 152 mmol, 1.16 eq) was dissolved in methanol (100 mL) and heated to 60 °C. Thioacetic acid (9.72 mL, 138 mmol, 1.06 eq) was added dropwise and subsequently, 4-vinylbenzyl chloride (18.5 mL, 131 mmol) was added slowly. The reaction mixture was stirred under reflux conditions for 2 h. After cooling the mixture down to room temperature, the solids were removed by filtration and washed with methanol and the filtrate was concentrated under reduced pressure. After addition of dichloromethane (100 mL), the solution was washed with water (3 × 100 mL). Silica column chromatography (*n*-heptane and ethyl acetate (90:10) as eluent) resulted in a colorless liquid (14.1 g, 56% yield). ^{1}H NMR (400 MHz, CDCl3) δ_H: 7.33–7.22 (m, 4H), 6.68 (dd, 1H), 5.72 (dd, 1H), 5.23 (dd, 1H), 4.11 (s, 2H), 2.35 (s, 3H). ^{13}C NMR (100 MHz, CDCl3) δ_C: 195.3, 137.3, 136.8, 136.5, 129.2, 126.6, 118.8, 33.4, 30.5.

Synthesis of 2-naphthyl acrylate (5). A solution of acryloyl chloride (2.3 mL, 28 mmol, 1.0 eq) in dichloromethane (10 mL) was added slowly under nitrogen atmosphere to a stirred solution of 2-naphthol (4.0 g, 28 mmol) and triethylamine (5.0 mL, 36 mmol, 1.3 eq) in dichloromethane (20 mL). The mixture was stirred for 2 h. Water (6 mL) was added to neutralize any remaining methacryloyl chloride. Subsequently, the mixture was extracted with dichloromethane (40 mL) and washed with brine (2 × 40 mL). The organic phases were combined and dried over $MgSO_4$ and concentrated under reduced pressure. Following silica column chromatography (*n*-heptane and ethyl acetate (90:10) as eluent) a white solid was obtained (3.33 g, 60% yield).

^{1}H NMR (400 MHz, CDCl3) δ_H: 7.85 (m, 3H), 7.62 (m, 1H), 7.49 (m, 2H), 7.28 (dd, 1H), 6.67 (dd, 1H), 6.39 (dd, 1H), 6.06 (s, 1H). ^{13}C NMR (100 MHz, CD (100 MHz, CDCl3) δ_C: 164.9, 148.3, 133.8, 132.9, 131.6, 129.6, 128.1, 127.9, 127.8, 126.7, 125.9, 121.2, 118.7.

Synthesis of poly(2-(ethyl xanthate)ethyl methacrylate — methyl methacrylate) [XAMA-MMA], poly(2-(ethyl xanthate) ethyl methacrylate — benzyl methacrylate) [XAMA-BMA] and poly(2-(ethyl thioacetate methacrylate — methyl methacrylate) [TAMA-MMA] copolymers (P1 + P2 + P3). Monomer **1** and **2** (XAMA and TAMA) were copolymerized with methyl methacrylate (MMA, **P1** and **P3**) or respectively benzyl methacrylate (BzMA, **P2**) in molar ratios of 1:20, 1:10 or 1:5. For example, monomer **1** (0.40 g, 1.71 mmol), methyl methacrylate (1.60 g, 15.98 mmol) 2-cyano-2-propyl benzodithioate (11.0 mg, 0.050 mmol, stock solution in chlorobenzene, 100 g/L) and AIBN (1.63 mg, 0.010 mmol, stock solution in chlorobenzene, 10 g/L) were combined with chlorobenzene (2 mL) in a polymerization flask fitted with a rubber septum. After purging for 10 min with nitrogen, the flask was heated in an oil bath at 70 °C. After 24 h, dichloromethane (2 mL) was added to the cooled flask and the polymer was precipitated in *n*-heptane.

P1: ^{1}H NMR (400 MHz, $CDCl_3$) δ_H: 4.73–4.63 (br, q, CH_2), 4.26–4.13 (br, t, CH_2), 3.70–3.52 (br, s, CH_3), 3.46–3.37 (br, t, CH_2), 2.09–1.74 (br), 1.49–1.39 (br), 1.25–1.19 (br), 1.06–0.97 (br), 0.89–0.74 (br).

P2: ^{1}H NMR (400 MHz, $CDCl_3$) δ_H: 7.38–7.22 (br, m, ArH), 5.02–4.80 (br, s, CH_2), 4.68–4.56 (br, q, CH_2), 4.22–3.99 (br, t, CH_2), 3.40–3.17 (br, t, CH_2), 2.19–1.51 (br), 1.49–1.28 (br), 1.18–1.09 (br), 1.07–0.85 (br), 0.85–0.52 (br).

P3: ^{1}H NMR (400 MHz, $CDCl_3$) δ_H: 4.11–4.02 (br t, CH_2), 3.67–3.55 (br s, CH_3), 3.21–3.11 (br t, CH_2), 2.41–2.37 (br s, CH_3), 2.09–1.74 (br), 1.49–1.35 (br), 1.34–1.18 (br), 1.06–0.97 (br), 0.90–0.79 (br).

Synthesis of poly(2-(ethyl thioacetate acrylate — methyl acrylate) [TAA-MA] and poly(4-vinylbenzyl thioacetate — styrene) [TASty-Sty] copolymers (P4 + P5). Monomer **3** and **4** (TAA and TASty) were copolymerized with methyl acrylate (MA, **P4**) or respectively styrene (Sty, **P5**) in a molar ratio of 1:10. For example, monomer **4** (0.64 g, 3.35 mmol), styrene (3.15 g, 30.25 mmol), 2-(butylthiocarbonothioylthio)propionic acid (5.00 mg, 0.021 mmol, stock solution in chlorobenzene, 100 g/L) and AIBN (0.69 mg, 0.004 mmol, stock solution in chlorobenzene, 10 g/L) were combined with 4 mL of chlorobenzene in a polymerization flask fitted with a rubber septum. After purging for 10 min with nitrogen, the flask was heated in an oil bath at 70 °C. After 16 h (**P4**) or 24 h (**P5**), dichloromethane (5 mL) was added to the cooled flask. **P4** was precipitated into *n*-heptane and **P5** was twice precipitated into methanol.

P4: ^{1}H NMR (400 MHz, $CDCl_3$) δ_H: 4.24–4.06 (br, t, CH_2), 3.75–3.57 (br, s, CH_3), 3.17–3.07 (br, t, CH_2), 2.42–2.22 (br, s, CH_3) overlapping with 2.37–2.33 (br), 1.99–1.85 (br), 1.82–1.36 (br).

P5:^{1}H NMR (400 MHz, $CDCl_3$) δ_H: 7.28–6.70 (br, m, ArH), 6.70–6.25 (br, m, ArH), 4.13–3.94 (br, s, CH_2), 2.38–2.25 (br, s, CH_3), 2.11–1.19 (br, m).

General procedures for thiol aminolysis of the copolymers. **P1** (500 mg, 0.44 mmol equiv. thiol monomer) was dissolved in THF (10 mL) and purged with nitrogen for 10 min in a sealed round-bottom flask. Under nitrogen flow, hydrazine (42.7 μL, 0.88 mmol, 2.00 eq) was added. The solution was stirred for 30 min in the case of **P1** and **P2**, 3 h for **P3** + **P4** and 24 h in the case of **P5**. Copolymer solutions were filtered and immediately used in nanoparticle formation. For ^{1}H NMR measurements, the polymer was precipitated into *n*-heptane (**P1**-**P4**) or methanol (**P5**).

P1: ^{1}H NMR (400 MHz, $CDCl_3$) δ_H: 4.16–4.04 (br t, CH_2), 3.70–3.52 (br, s, CH_3), 2.83–2.72 (br, t, CH_2), 2.09–1.49 (br), 1.49–1.39 (br), 1.25–1.19 (br), 1.09–0.95 (br), 0.89–0.79 (br).

P2: ^{1}H NMR (400 MHz, $CDCl_3$) δ_H: 7.38–7.22 (br, ArH), 5.02–4.80 (br, s, CH_2), 4.05–3.87 (br, t, CH_2), 2.72–2.51 (br, t, CH_2), 2.19–1.51 (br), 1.49–1.28 (br), 1.18–1.09 (br), 1.07–0.85 (br), 0.85–0.52 (br).

P3: ^{1}H NMR (400 MHz, $CDCl_3$) δ_H: 4.15–4.06 (br t, CH_3), 3.67–3.55 (br s, CH_3), 2.83–2.73 (br t, CH_2), 2.09–1.74 (br), 1.49–1.35 (br), 1.34–1.18 (br), 1.06–0.97 (br), 0.90–0.79 (br).

P4: ^{1}H NMR (400 MHz, $CDCl_3$) δ_H: 4.28–4.11 (br, t, CH_2), 3.75–3.57 (br, s, CH_3), 2.80–2.71 (br, t, CH_2), 2.42–2.22 (br), 1.99–1.85 (br), 1.82–1.36 (br).

P5: ^{1}H NMR (400 mHz, $CDCl_3$) δ_H: 7.28–6.70 (br, m, ArH), 6.70–6.25 (br, m, ArH), 3.75–3.58 (br, s, CH_2), 2.11–1.19 (br, m).

Xanthate nanoparticle formation (NP1, NP1-N, NP2, NP3, NP4). In a 3-necked round bottom flask, equipped with dropping funnel, dichloromethane (100 mL) was purged with nitrogen. Subsequently, 1,4-butanediol diacrylate (82.7 μL, 44 mmol, 1.00 eq) and a catalytic amount of tri(*n*-butyl) phosphine (19.8 μL, 0.08 mmol, 0.18 eq) were added to the purged dichloromethane. The solution of deprotected copolymer (500 mg) in THF (10 mL)

was dropwise added to the continuously stirred cross-linker solution over 30 min. After stirring for an additional 2 h, 2.6 mL methyl acrylate (24 mmol) or respectively 1.1 g of monomer **5** (5 mmol), was added to react with any remaining thiols and the solution was left stirring overnight. In case of labeling with monomer **5** (**NP1-N**), 2 mL of methyl acrylate (20 mmol) was added the next morning to react 1 additional hour. After concentrating the solution under reduced pressure and addition of 5 mL methanol to **NP1**, the nanoparticles were precipitated. **NP1**, a white powder, was isolated by precipitation in diethyl ether followed by centrifugation (for **NP1**), whereas **NP2** was obtained through precipitation in *n*-heptane, followed by precipitation in methanol. **NP3** and **NP4** were precipitated into *n*-heptane. (150 mg).

NP1: ^{1}H NMR (400 MHz, $CDCl_3$) δ_H: 4.25–4.04 (br, t, CH_2), 3.68–3.52 (br, s, CH_3), 3.06–2.71 (br, CH_2), 2.70–2.59 (br, CH_2), 2.54–2.38 (br, CH_2), 2.09–1.33 (br), 1.26–1.19 (br), 1.12–0.94 (br), 0.93–0.71 (br).

NP1-N: ^{1}H NMR (400 MHz, $CDCl_3$) δ_H: 7.90–7.77 (br m), 7.60–7.55(br), 7.53–7.44 (br m), 7.26–7.20 (br), 4.25–4.04 (br, t, CH_2), 3.68–3.52 (br, s, CH_3), 3.06–2.71 (br, CH_2), 2.70–2.59 (br, CH_2), 2.54–2.38 (br, CH_2), 2.09–1.33 (br), 1.26–1.19 (br), 1.12–0.94 (br), 0.93–0.71 (br).

NP2: ^{1}H NMR (400 MHz, $CDCl_3$) δ_H: 7.38–7.22 (br, ArH), 5.02–4.80 (br, s, CH_2), 4.22–3.90 (br, t, CH_2), 3.76 (s, CH_3), 2.95–2.55 (br, CH_2), 2.53–2.43 (br, CH_2), 2.19-1.49-1.28 (br), 1.18–1.09 (br), 1.07–0.85 (br), 0.85–0.52 (br).

NP3: ^{1}H NMR (400 MHz, $CDCl_3$) δ_H: 4.25–4.06 (br t, CH_3), 3.67–3.55 (br s, CH_3), 3.06–2.71 (br, CH_2), 2.70–2.60 (br, CH_2), 2.54–2.40 (br, CH_2), 2.09–1.35 (br), 1.34–1.18 (br), 1.10–0.95 (br), 0.93–0.75 (br).

NP4: ^{1}H NMR (400 MHz, $CDCl_3$) δ_H: 4.28–4.09 (br, t, CH_2), 3.75–3.57 (br, s, CH_3), 2.86–2.79 (t, CH_2), 2.79–2.71 (br, t, CH_2), 2.67–2.60 (t, CH_2), 2.54–2.43 (br), 2.42–2.22 (br), 1.99–1.85 (br), 1.82–1.36 (br).

4-Vinylbenzyl thioacetate nanoparticle formation (NP5). In a 3-necked round bottom flask, equipped with dropping funnel, dichloromethane (100 mL) was purged with nitrogen. Subsequently, 1,4-butanediol diacrylate (83.1 μL, 0.44 mmol) and a catalytic amount of tri(n-butyl) phosphine (19.9 μL, 0.81 mmol, 0.18 eq) were added to the purged dichloromethane. The deprotected copolymer was dissolved in 10 mL THF and was added to the continuously stirred cross-linker solution dropwise over 30 min. After stirring for an additional 4 h, a) methyl acrylate (3.0 mL, 28.06 mmol) or b) 2-(dimethylaminoethyl) acrylate (3.0 mL, 19.61 mmol) was added to react with any remaining thiols. The solution was left stirring overnight. After concentrating the solution under reduced pressure to 10 mL, the nanoparticles were precipitated in methanol and centrifuged. For ^{1}H NMR measurements, the nanoparticles were precipitated in *n*-heptane. (100 mg).

NP5a: ^{1}H NMR (400 MHz, CDCl3) δ: 7.26–6.22 (br, m, ArH), 4.51–4.32 (br), 4.24–4.04 (br, CH_2), 3.88–3.52 (br s, CH_2), 3.00–2.75 (br, CH_2), 2.75–2.40 (br, CH_2), 2.26–1.10 (br, m).

NP5b: ^{1}H NMR (400 MHz, CDCl3) δ: 7.26–6.22 (br, m, ArH), 4.25–4.16 (br), 3.71–3.52 (br, s, CH_2), 2.71–2.40 (br, CH_2), 2.26–1.10 (br, m).

3. Results and discussion

3.1. Monomer and copolymer synthesis

For the preparation of well-defined thiol-functional polymers, a xanthate methacrylate monomer (**1**) was synthesized following a 2-step literature procedure and copolymerized together with either MMA (**P1**) or BzMA (**P2**) via RAFT polymerization. The theoretical molecular weight was calculated based on monomer conversion as observed by ^{1}H NMR spectroscopy (Table 1). GPC (gel permeation chromatography) data confirmed polymer molecular weights were close to the targeted molecular weights, with low polydispersities (PDI ~ 1.1). A second polymer thiol system was prepared from thioacetate monomers (**2**, **3, 4**) to yield copolymers (**P3-P5**). Ethyl thioacetate methacrylate (**2**) was synthesized based on potassium thioacetate, similar to monomer **1**, whereas 4-vinyl benzyl thioacetate (**4**) was obtained through nucleophilic substitution of vinyl benzyl chloride with thioacetic acid [62]. Through RAFT polymerization of **2, 3**, **4** with MMA, MA and styrene respectively, polymer precursors with the targeted molecular weights and generally low polydispersities (PDI ~ 1.2) were obtained (Table S1). For all polymers, monomer incorporation ratios were in good agreement with the feed ratios.

3.2. Thiol deprotection

Before nanoparticles were prepared from the polymers, thiol moieties were deprotected via aminolysis with hydrazine (Scheme 1). Hydrazine was chosen for the aminolysis, since it can rapidly cleave the thiol protecting groups, but also because of its strong reducing properties preventing possible disulfide formation [64]. Complete aminolysis of xanthate moieties for copolymers **P1** and **P2** was confirmed by ^{1}H NMR spectroscopy, as the *O*-ethyl signals at 4.6 ppm vanished (signal c, Fig. 3), while the CH_2 group adjacent to the sulfur shifted from 3.3 to 2.6 ppm (signal b, Fig. 3). The ^{1}H NMR studies of the aminolysis step did not reveal significant differences between hydrazine (2 equivalents) in THF and *n*-butylamine (4 equivalents) in DMF, neither in reaction kinetics, nor in reaction products.

When comparing FTIR spectra of **P1** before and after deprotection, the strong signal at 1045 cm^{-1}, which is attributed to C=S stretching vibrations, is drastically diminished (Fig. S1). Furthermore, decreasing absorptions at 1112 and 1237-1223 cm^{-1} in the area of C-O-C stretching vibrations were observed. A very weak signal at 2572 cm^{-1} indicates the presence of thiols.

The aminolysis of the ethyl thioacetate moieties of **P3**, **P4** and **P5**

Table 1
Comparison of molecular weights of xanthate copolymers with different chain lengths and their corresponding nanoparticles.

			$M_{n,theo}$ [a] Polymer (kg·mol^{-1})	$M_{w,GPC}$ [b] Polymer (kg·mol^{-1})	PDI [b] Polymer	χ_{SH}	M_w [b] SCNP (kg·mol^{-1})	PDI [b] SCNP	ΔM_W [c]	$r_{H,GPC}$ [d] Polymer (nm)	$r_{H,GPC}$ [d] SCNP (nm)	$r_{H,DLS}$ [e] SCNP (nm)
MMA (**P1**)	Chain length variation	**P1a**	32.0	35.5	1.06	10%	15.8	1.29	55%	5.1	3.3	3.3
		P1b	47.4	50.1	1.05	10%	17.7	1.52	65%	6.2	3.5	3.8
		P1c	101.0	96.0	1.15	10%	21.7	1.62	77%	9.0	3.9	4.9
BzMA (**P2**)	Chain length variation	**P2a**	57.6	26.3	1.14	9%	20.9	1.33	21%	4.3	3.8	4.1
		P2b	92.0	43.2	1.16	10%	23.5	1.41	46%	5.7	4.1	6.9
		P2c	165.7	97.6	1.30	9%	10.3	3.58	89%	9.1	2.6	9.1

[a] Estimated through ^{1}H NMR. [b] Determined by GPC, relative to polystyrene standards. [c] Reduction in apparent weight-average molecular weight, calculated as $((M_{W,SCNP} - M_{w,Pol})/M_{W,SCNP}) \cdot 100\%$. [d] $r_H = 1.44 \cdot 10^{-2} \cdot (M_{W,GPC})^{0.561}$ [66]. [e] Measured in chloroform.

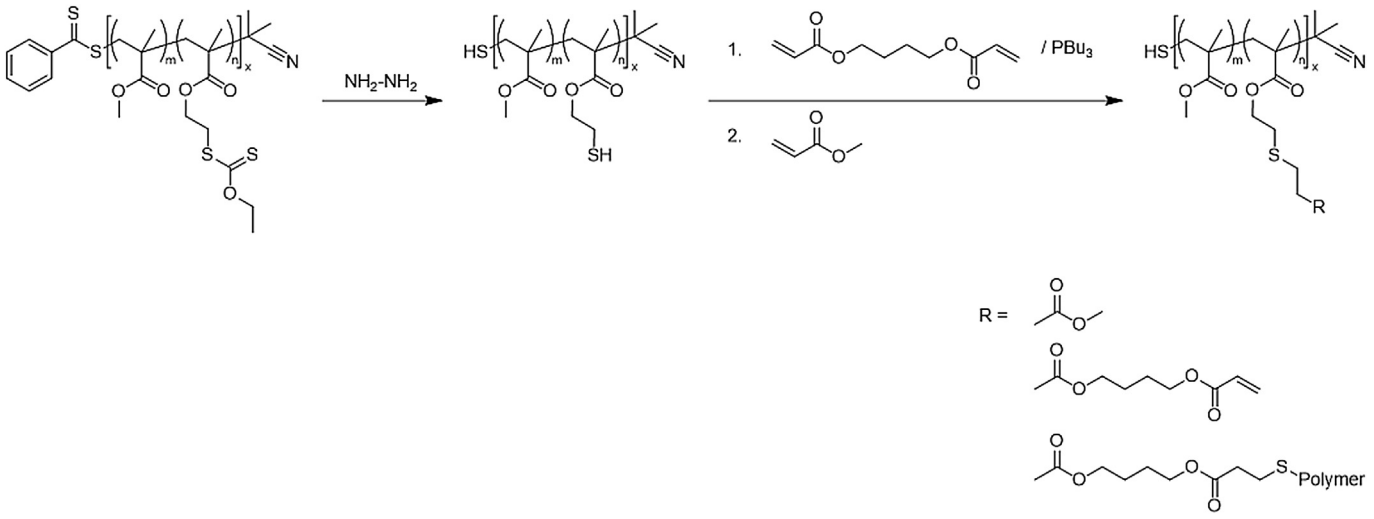

Scheme 1. Aminolysis of xanthate copolymer **P1** and synthesis of single-chain nanoparticles **NP1.**

was tracked via ^{1}H NMR spectroscopy through the disappearance of the methyl ketone peaks at 2.3–2.4 ppm (signal c, Fig. S6). Furthermore, the ethyl peak shift from 3.1 to 2.8 ppm for **P3** and **P4** and from 4.0 to 3.6 ppm for **P5** in ^{1}H NMR measurements (signal b, Fig. S6). The FTIR spectrum of **P5** gives additional evidence for a successful deprotection of the thioacetate group through the significant disappearance of the thioester carbonyl band at 1691 cm^{-1} (Fig. S2).

Whereas the aminolysis step is rather fast for the xanthate ester polymers **P1** and **P2** (below 30 min) and slightly slower for the ethyl thioacetate polymers **P3** and **P4** (3 h), the deprotection of thioacetate styrene polymers **P5** took 24 h. Hydrolysis of **P5** with hydrochloric acid (1 M in methanol) as an alternative deprotection method proved even slower (57% deprotection after 24 h), than the deprotection by aminolysis. The difference in aminolysis rates for ethyl xanthate and ethyl thioacetate confirms that alkyl thioacetates are less electrophilic and hence less reactive than xanthates [60]. However, the significantly longer reaction times observed for thioactetate styrene as compared to the ethyl thioacetates may be caused by increased steric hindrance of the thiols in **P5**. Accordingly, longer reaction times for cross-linking and thiol capping were employed for **P5**.

3.3. Preparation of single-chain polymer nanoparticles

Without further purification, the deprotected thiol-functional polymer THF solution was slowly added to the cross-linker solution in CH_2Cl_2, containing phosphine catalyst, in order to prepare

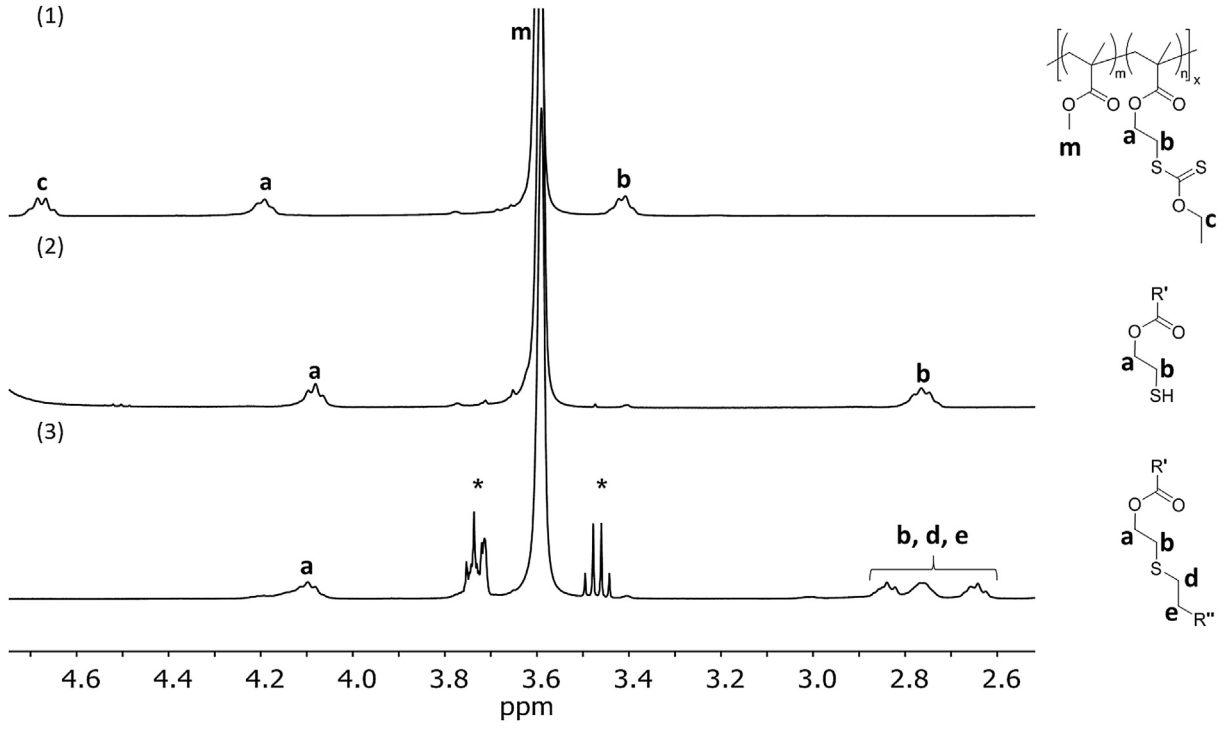

Fig. 3. ^{1}H NMR spectra of (1) protected precursor polymer **P1**, (2) deprotected polymer and (3) nanoparticle **NP1**. * residual solvent signals: diethyl ether and tetrahydrofuran.

SCNPs. To avoid polymer-polymer coupling, a slow addition rate was chosen (i.e. 0.5 mL/min). Finally, methyl acrylate was added after polymer addition was complete to react with remaining thiol moieties and to prevent future side reactions and cross-linking (Scheme 1).

The thiol-Michael addition crosslinking can be observed by ^{1}H NMR spectroscopy for all polymers (**P1**-**P5**), as peaks of the thiol-ene coupling occur between 2.4 and 2.9 ppm and additionally alkoxy signals appear at 4.0 ppm (Fig. 3, Figs. S3-S6). Moreover, the successful thiol-Michael addition product results in signals between 4.1 and 4.2 ppm in the ^{1}H NMR spectrum from the butylene ester groups of the cross-linker. However, due to overlapping signals, ^{1}H NMR spectroscopy neither enables distinguishing between thiol capping and cross-linking in this case, nor between intra- and intermolecular cross-linking. In addition, acrylate peaks between 5.8 and 6.5 ppm indicate that also monoaddition of the cross-linker occurs.

To gain information about the hydrodynamic radii of the SCNPs dynamic light scattering (DLS) measurements were performed. DLS measurements in chloroform support the presence of 10 nm species for all nanoparticles. However, the random coiled linear polymer chains and single-chain nanoparticles do not necessarily differ significantly in size (Fig. S16). Furthermore, DLS data showed additional species above 100 nm in size for both polymers and nanoparticles that influenced the quality of the measurements, especially for measurements of **P1** and **NP1**. This peak was not stable through the measurements and occurs therefore only intermittently. The peak is attributed to the interaction between polymers and the solvent [65]. Both **P2** polymers and **NP2** nanoparticles display much less aggregation behavior, but rather more pronounced size differences between polymers and nanoparticles (Fig. S17). Possibly, the DLS measurements were affected by polymer and nanoparticle agglomerates in solution that appear at higher sizes.

GPC shows drastic changes between the precursor polymers and the resulting nanoparticles (Table 1 and Table S1). Methyl methacrylate copolymers **P1** and **P3** show comparable size reductions between 60 and 70% for 40–50 kDa precursor lengths. **P4** and **P5** display a reduction of approximately 45% for polymers in the same size range. These differences in relative size reduction between styrene and the (meth)acrylates copolymers may be caused by differences in the hydrodynamic volume due to polarity. Hydrodynamic radii of the nanoparticles were calculated from the M_w values obtained from GPC analysis, revealing overall agreement with the radii obtained from DLS measurements [66,67].

Decreases in apparent molecular weights of the cross-linked polymers between 30 and 90% as observed by GPC measurements in combination with ^{1}H NMR spectroscopy measurements confirm successful intramolecular cross-linking. The GPC values should not be understood as absolute values, but as apparent molecular weights relative to the external calibration. As can be seen in the substantial discrepancies in molecular weights estimated through GPC and NMR (Table 1), GPC can only give molecular weight values, and therefore changes in hydrodynamic radius, in comparison to polystyrene standards.

To validate whether the observed molecular weight changes were caused by reduction in hydrodynamic radius or by changes in polarity in the final nanoparticle structure (owing to the cross-linker and deprotected thiol moieties), **P1** was also functionalized by reacting the thiol moieties with excess methyl acrylate. The GPC traces of native copolymer **P1** and the methyl acrylate functionalized copolymer **P1MA** did not display significant differences (Fig. S13). Hence, the decreases in apparent molecular weight are assigned to intramolecular cross-links, which reduce the degrees of freedom of the polymer chains and concomitantly its occupied volume (hydrodynamic radius). In order to verify whether the polymer concentration is sufficiently low to prevent intermolecular crosslinking, nanoparticle formation was also performed under higher dilution. However, two-fold dilution did not result in noticeable additional reductions in particle size as verified by GPC (Fig. S14).

Particle size dependence on precursor polymer length and cross-linker ratio.

The relationship between precursor polymer and resulting nanoparticle was evaluated by varying the lengths (molecular weights) of the precursors, **P1** and **P2**, and comparing the resulting nanoparticles by GPC (Table 1, Fig. 4 and Fig. S9).

While the short **P1a** polymer (Mw = 30 kDa) decreased 55% in size, the medium length polymer (**P1b**, Mw = 50 kDa) decreased 65%, and the largest polymer (**P1c**, Mw = 100 kDa) decreased up to 77% in hydrodynamic radius. For **P2**, the changes in hydrodynamic radius are more pronounced: while the short **P2a** polymer (Mw = 30 kDa) decreased approximately 20% in size, the largest polymer (**P2c**, Mw = 100 kDa) decreased even up to 90% in hydrodynamic radius. When taking into account the monomer molecular weight employed in the different polymers, i.e. MMA and BzMA for **P1** and **P2** respectively, excellent agreement is observed for the size reductions (Fig. 5a and Fig. S15). Provided the formed SCNPs are indeed composed of single polymer chains, particle size is directly dependent on the precursor chain length. A comparison of GPC data of SCNPs with varying molecular weights indeed displays a more pronounced reduction in apparent molecular weight with increasing precursor polymer chain length. The length-dependent size reduction is caused by more possibilities for intramolecular cross-links due to the presence of more cross-linkable groups along the polymer chain.

Similarly, a comparison was made of the size reductions observed for particles prepared from **P2** polymers with different xanthate fractions (5%, 10%, 20%), while maintaining molecular weight constant between 30 and 40 kDa (Fig. 5b, Table 2). A low content of cross-linkable units (5%) in **P2** resulted in a 30% size reduction, whereas 20% cross-linkable units resulted in a 76% reduction in apparent molecular weight.

As the total number of cross-linkable groups per polymer increases, either due to polymer length or thiol fraction, polydispersities of the SCNPs increase markedly. This effect is a result of the increasing number of potential conformations of the SCNPs. **P2c**, especially, suggests a distribution of several collapsed states.

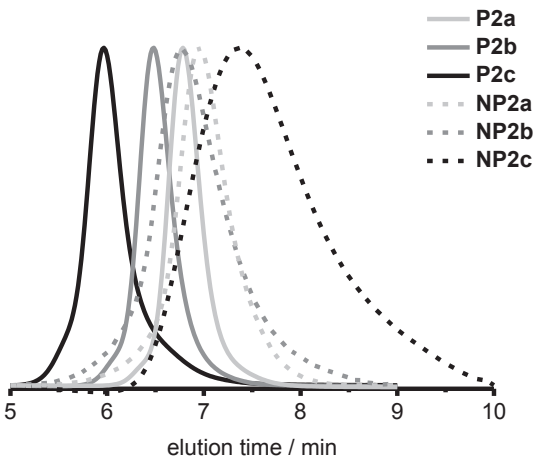

Fig. 4. Overlay of GPC traces for the BzMA-XanthateMA copolymer precursors (**P2a-c**) with different chain lengths and their corresponding nanoparticles (**NP2a-c**).

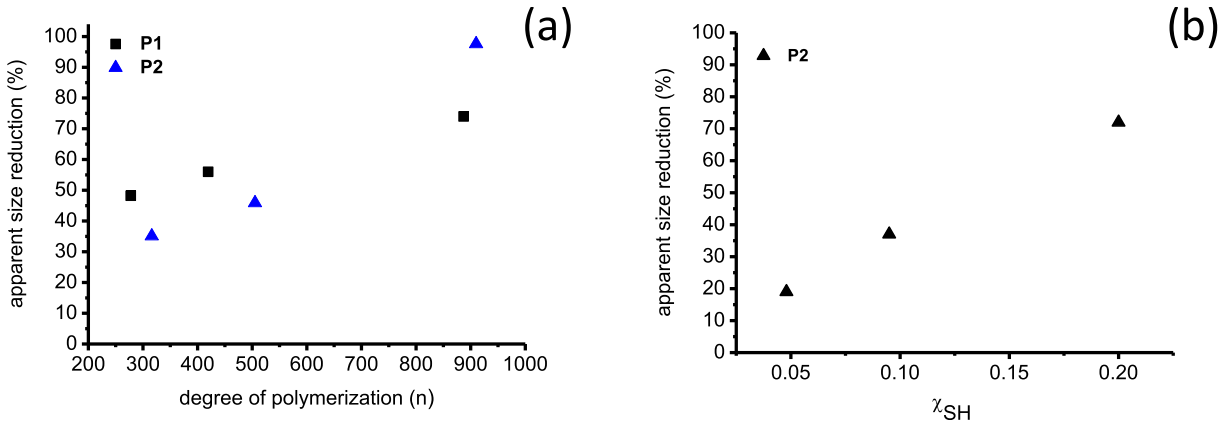

Fig. 5. Plots of apparent size reduction of the SCNP versus (a) the degree of polymerization and (b) the thiol content of the precursor polymers.

Table 2
Comparison of molecular weights of **P2** with different composition with their corresponding nanoparticles.

		x_{SH}	$M_{n,theo}$ [a] Polymer (kg·mol^{-1})	$M_{w,GPC}$ [b] Polymer (kg·mol^{-1})	PDI [b] Polymer (kg·mol^{-1})	$M_{w,NP}$ [b] SCNP (kg·mol^{-1})	PDI [b] SCNP	ΔM_W [c]
BzMA	Thiol content variation	5%	68.8	43.4	1.22	30.6	1.66	30%
(P2)		10%	92.0	43.2	1.16	23.5	1.41	46%
		20%	67.1	32.5	1.16	7.9	–	76%

[a] Determined by ^{1}H NMR. [b] Determined by GPC, relative to polystyrene standards. [c] Reduction in apparent weight-average molecular weight, calculated as $((M_{W,SCNP} - M_{w,Pol})/M_{W,\ SCNP}) \cdot 100\%$.

Nanoparticles from 20% xanthate polymers were rather ill-defined and isolation was impeded.

3.4. Particle imaging

SCNP morphology was investigated by atomic force microscopy (AFM) on **NP1**, prepared from a 50 kDa polymer **P1** precursor and the three different sizes of cross-linked **P2** polymers (i.e. **NP2**). The particles imaged here in AFM were around 0.9 nm of height and around 30 nm in radius, which indicates that these SCNPs do not maintain a globular structure (Fig. 6 and Fig. S18), but the coils rather spread out on the surface as reported earlier [68,69]. Mackay and coworkers for example, observed that moderately cross-linked SCNPs collapse into a flat shape and lose their conformational entropy on a high-energy substrate surface such as mica [68]. Particle height and radius as observed by AFM were used to determine the dimensions of a spherical conformation in solution as proposed by Berda et al. [69] The observed structures correspond to 5–8 nm spherical particles (Table S3), which is in the same range as radii obtained from DLS and GPC (Table 1, Figs. S16–17). **NP1** displayed a radius of 40 nm and a height of 0.5 nm and hence, the AFM values can be related to spherical nanoparticles of 7.4 nm (Fig. 6). All three **NP2** nanoparticle species were below 10 nm in size, while the lowest molecular weight precursor polymer resulted in the smallest nanoparticle (5.6 nm).

Interestingly, the individual particles display a darkened core in the AFM phase image (Fig. 6b). Berda et al. observed a similar effect for reversible SCNPs and ascribed the darkened core to stacking interactions of the employed hydrogen-bonding cross-linking units [69]. Although the pattern is not an ideal round shape, it is already apparent in the polymer precursor (Fig. S19).

Scanning transmission electron microscopy (STEM) measurements on **NP2a** nanoparticles confirmed a radius of the surface adsorbed particles of approximately 20 nm (Fig. 7), which is in

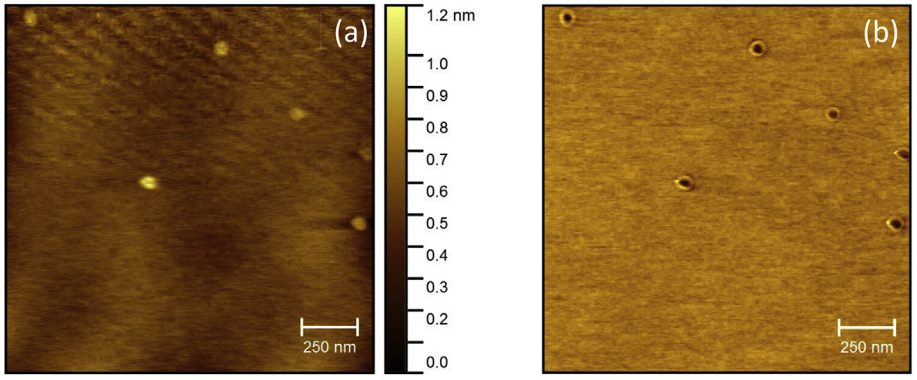

Fig. 6. AFM height (a) and phase (b) images of **NP1** nanoparticles.

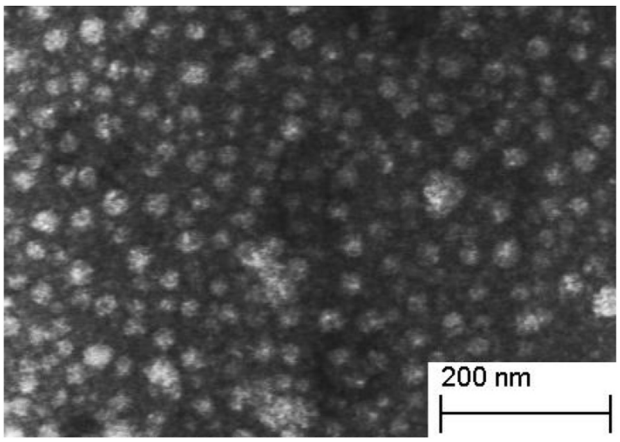

Fig. 7. STEM image of stained **NP2a.**

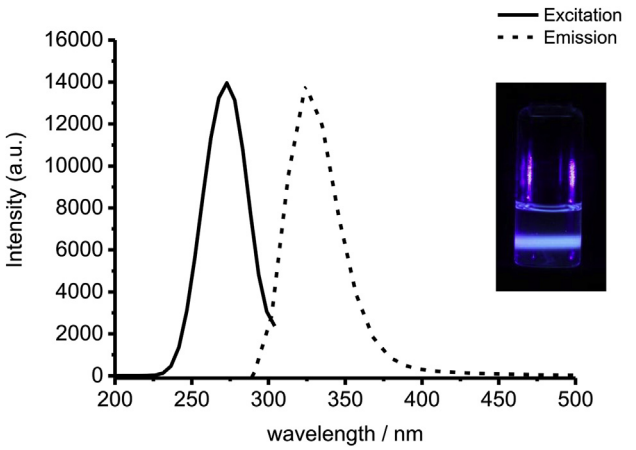

emission spectra of fluorescence detector (excitation at 270 nm).

Fig. 9. Fluorescence excitation and emission spectra of **NP1c-N** at 6.65 min elution time. The excitation spectrum was recorded at an emission at 324 nm and the sample was excited at 270 nm for the emission spectrum.

excellent agreement with AFM data ($r_{adsorbed}$ = 21 nm); a similar particle flattening as observed by AFM is likely occurring. As the height of the particles cannot be estimated with STEM, no further validation was performed.

3.5. Functionalization of SCNPs via monoacrylates

The endcapping step with monoacrylates may be exploited as a means to modify the nanoparticle surface. To demonstrate the versatility in endcapper use, **NP5** and **NP1c** were capped with different acrylates, i.e. *N,N*-dimethylaminoethyl acrylate and 2-naphthyl acrylate (monomer **5**).

The resulting **NP5** nanoparticles were isolated in the same way as methyl acrylate functionalized **NP5** and did not demonstrate any significant differences in GPC to the original system. The presence of the DMAEA was confirmed by the peaks at 4.21, 2.58 and 2.29 ppm in the ^{1}H NMR spectrum. Through DMAEA incooperation, positive charges, in the form of quaternary amine catium, may be introduced onto the nanoparticles.

Modification of SCNPs with 2-naphthyl acrylate (monomer **5**) was followed by exposure of the nanoparticles to methyl acrylate prior to their isolation to ensure that even sterically hindered thiols were capped. Distinct peaks of the naphthalene ring were observed in the ^{1}H NMR spectrum of **NP1c-N** confirming that substantial endcapping with monomer **5** took place (~25% of thiols, Fig. S7). The modification did not affect isolation of the nanoparticles and the size reduction in the GPC of the naphthyl-functionalized **NP1c-N** was comparable to those observed for SCNPs endcapped with methyl acrylate (Fig. 8). Importantly, the labeled nanoparticles displayed fluorescence signals in the GPC traces. The excitation and emission spectra of the nanoparticle peak, displayed an excitation maximum at 273 nm and an emission maximum at 324 nm, whereas the polymer does not show any significant fluorescence (Fig. 9).

4. Conclusions

Single-chain polymer nanoparticles were successfully prepared via intramolecular thiol-Michael addition between thiol polymers and bifunctional acrylates. Formation was confirmed by ^{1}H NMR spectroscopy and GPC, and nanoparticles were visualized by AFM and STEM. Size-controlled SCNPs were achieved by employing different polymer lengths and different fractions of thiols in the polymers. Besides providing modularity through monomer choice in the preparation of precursor polymers, residual thiol moieties can act as an additional handle for particle functionalization through the use of different endcappers. Thiol-Michael addition has thus been introduced as a robust and versatile approach to build

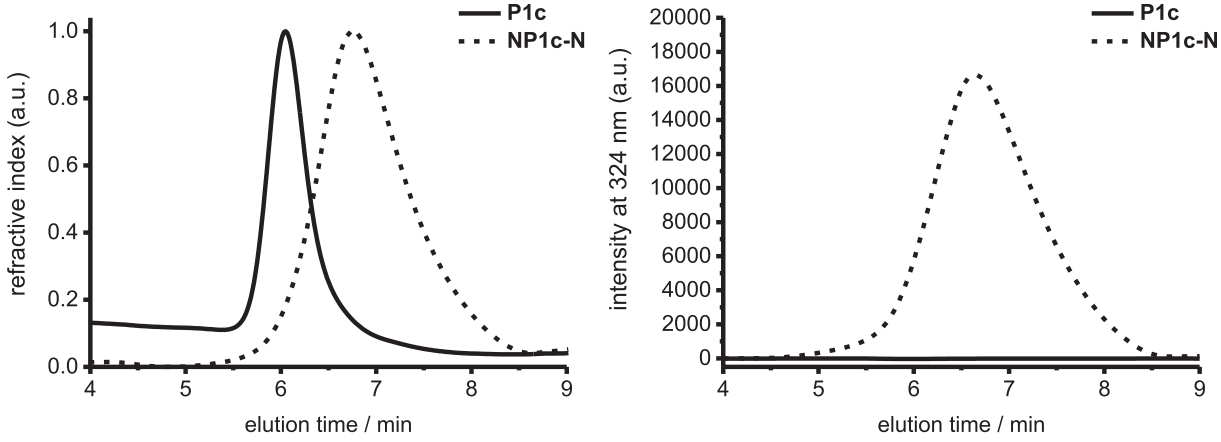

Fig. 8. Overlay of GPC traces for the MMA-XanthateMA copolymer precursor (**P1c**) and the corresponding 2-naphthyl-labeled nanoparticles (**NP1c-N**). Left: refractive index detector. Right: emission spectra of fluorescence detector (excitation at 270 nm).

well-defined SCNPs under benign conditions. Our current investigations focus on further extending the modularity of this promising class of materials, as well as exploring their potential in biomedical applications, such as drug delivery and imaging.

Acknowledgments

We gratefully acknowledge funding from the Netherlands Organisation for Health Research and Development (ZonMw, project number 733050304). We thank Mark Smithers for the STEM measurements, as well as Dr. ir. Martin Bennink and Kees van der Werf for support with the AFM measurements. Ir. Robbert van der Houwen is thanked for fruitful discussions and synthesis support.

Appendix A. Supplementary data

Supplementary data related to this article can be found at http://dx.doi.org/10.1016/j.polymer.2017.05.040.

References

[1] C.J. Hawker, K.L. Wooley, Science 309 (2005) 1200–1205.
[2] S. Perrier, P. Takolpuckdee, J. Polym. Sci. Part A Polym. Chem. 43 (2005) 5347–5393.
[3] K. Matyjaszewski, N.V. Tsarevsky, Nat. Chem. 1 (2009) 276–288.
[4] N. Anton, J.P. Benoit, P. Saulnier, J. Control. Release 128 (2008) 185–199.
[5] E. Lepeltier, C. Bourgaux, P. Couvreur, Adv. Drug Deliv. Rev. 71 (2014) 86–97.
[6] N. Mendoza-Munoz, D. Quintanar-Guerrero, E. Allemann, Recent Pat. Drug Deliv. Formul. 6 (2012) 236–249.
[7] R.C. Beck, A.F. Ourique, S.S. Guterres, A.R. Pohlmann, Recent Pat. Drug Deliv. Formul. 6 (2012) 195–208.
[8] A. Khan, M. Malkoch, M.F. Montague, C.J. Hawker, J. Polym. Sci. Part A Polym. Chem. 46 (2008) 6238–6254.
[9] H. Gao, W. Li, K. Matyjaszewski, Macromolecules 41 (2008) 2335–2340.
[10] S.C. Thickett, R.G. Gilbert, Polym. Guildf. 48 (2007) 6965–6991.
[11] R. Srikar, A. Upendran, R. Kannan, Wiley Interdiscip. Rev. Nanomedicine Nanobiotechnol. 6 (2014) 245–267.
[12] J.E. Dahlman, C. Barnes, O.F. Khan, A. Thiriot, S. Jhunjunwala, T.E. Shaw, Y. Xing, H.B. Sager, G. Sahay, L. Speciner, et al., Nat. Nanotechnol. 9 (2014) 648–655.
[13] Y. Gao, V.I. Böhmer, D. Zhou, T. Zhao, W. Wang, J.M.J. Paulusse, J. Control. Release 244 (2016) 375–383.
[14] M. Elsabahy, K.L. Wooley, Chem. Soc. Rev. 41 (2012) 2545–2561.
[15] E. Blanco, H. Shen, M. Ferrari, Nat. Biotechnol. 33 (2015) 941–951.
[16] N. Kamaly, Z. Xiao, P.M. Valencia, A.F. Radovic-Moreno, O.C. Farokhzad, Chem. Soc. Rev. 41 (2012) 2971–3010.
[17] Q. Fu, E.H.H. Wong, J. Kim, J.M.P. Scofield, P.A. Gurr, S.E. Kentish, G.G. Qiao, J. Mater. Chem. A 2 (2014) 17751–17756.
[18] A. Halim, Q. Fu, Q. Yong, P.A. Gurr, S.E. Kentish, G.G. Qiao, J. Mater. Chem. A 2 (2014) 4999–5009.
[19] S. Tan, Q. Fu, J.M.P. Scofield, J. Kim, P.A. Gurr, K. Ladewig, A. Blencowe, G.G. Qiao, J. Mater. Chem. A 3 (2015) 14876–14886.
[20] J. Zhu, Y. Zhang, M. Tian, J. Liu, ACS Sustain. Chem. Eng. 3 (2015) 690–701.
[21] S. Zhao, Z. Wang, J. Wang, S. Yang, S. Wang, J. Memb. Sci. 376 (2011) 83–95.
[22] A. Albanese, P.S. Tang, W.C. Chan, Annu. Rev. Biomed. Eng. 14 (2012) 1–16.
[23] H.S. Choi, W. Liu, P. Misra, E. Tanaka, J.P. Zimmer, B. Itty Ipe, M.G. Bawendi, J. V Frangioni, Nat. Biotechnol. 25 (2007) 1165–1170.
[24] X. Liang, H. Wang, Y. Zhu, R. Zhang, V.C. Cogger, X. Liu, Z.P. Xu, J.E. Grice, M.S. Roberts, ACS Nano 10 (2016) 387–395.
[25] H.H. Gustafson, D. Holt-Casper, D.W. Grainger, H. Ghandehari, Nano Today 10 (2015) 487–510.
[26] M. Longmire, P.L. Choyke, H. Kobayashi, Nanomedicine 3 (2008) 703–717.
[27] M. Antonietti, T. Nestl, Macromol. Rapid Commun. 15 (1994) 111–116.
[28] K. Zhang, Z. Gui, D. Chen, M. Jiang, Chem. Commun. 7 (2009) 6234–6236.
[29] L. Li, A. Chang, Y. Hu, L. Zhang, W. Wu, Chem. Commun. 49 (2013) 6534–6536.
[30] M. Chen, W. Yang, M. Yin, Small 9 (2013) 2715–2719.
[31] M.K. Aiertza, I. Odriozola, G. Cabañero, H.-J. Grande, I. Loinaz, Cell. Mol. Life Sci. 69 (2012) 337–346.
[32] S. Mavila, O. Eivgi, I. Berkovich, N.G. Lemcoff, Chem. Rev. 116 (2016) 878–961.
[33] W. Kuhn, G. Balmer, J. Polym. Sci. 57 (1962) 311–319.
[34] G. Allen, J. Burgess, S.F. Edwards, D.J. Walsh, Proc. R. Soc. A Math. Phys. Eng. Sci. 334 (1973) 477–491.
[35] J.E. Martin, B.E. Eichinger, Macromolecules 16 (1983) 1350–1358.
[36] A.M. Hanlon, C.K. Lyon, E.B. Berda, Macromolecules 49 (2016) 2–14.
[37] E. Harth, B. Van Horn, V.Y. Lee, D.S. Germack, C.P. Gonzales, R.D. Miller, C.J. Hawker, J. Am. Chem. Soc. 124 (2002) 8653–8660.
[38] J.B. Beck, K.L. Killops, T. Kang, K. Sivanandan, A. Bayles, M.E. Mackay, K.L. Wooley, C.J. Hawker, Macromolecules 42 (2009) 5629–5635.
[39] A. Sanchez-Sanchez, I. Pérez-Baena, J.A. Pomposo, Molecules 18 (2013) 3339–3355.
[40] J. He, L. Tremblay, S. Lacelle, Y. Zhao, Soft Matter 7 (2011) 2380–2386.
[41] A.E. Cherian, F.C. Sun, S.S. Sheiko, G.W. Coates, J. Am. Chem. Soc. 129 (2007) 11350–11351.
[42] A. Prasher, C.M. Loynd, B.T. Tuten, P.G. Frank, D. Chao, E.B. Berda, J. Polym. Sci. Part A Polym. Chem. 54 (2016) 209–217.
[43] A. Sanchez-Sanchez, J.A. Pomposo, Part. Part. Syst. Charact. 31 (2014) 11–23.
[44] M. Seo, B.J. Beck, J.M.J. Paulusse, C.J. Hawker, S.Y. Kim, Macromolecules 41 (2008) 6413–6418.
[45] E.J. Foster, E.B. Berda, E.W. Meijer, J. Am. Chem. Soc. 131 (2009) 6964–6966.
[46] A. Sanchez-Sanchez, A. Arbe, J. Colmenero, J.A. Pomposo, ACS Macro Lett. 3 (2014) 439–443.
[47] C.K. Lyon, A. Prasher, A.M. Hanlon, B.T. Tuten, C.A. Tooley, P.G. Frank, E.B. Berda, Polym. Chem. 6 (2015) 181–197.
[48] I. Perez-Baena, I. Asenjo-Sanz, A. Arbe, A.J. Moreno, F. Lo Verso, J. Colmenero, J.A. Pomposo, Macromolecules 47 (2014) 8270–8280.
[49] B.T. Tuten, D. Chao, C.K. Lyon, E.B. Berda, Polym. Chem. 3 (2012) 3068.
[50] C. Song, L. Li, L. Dai, S. Thayumanavan, Polym. Chem. 6 (2015) 4828–4834.
[51] A. Sanchez-Sanchez, S. Akbari, A. Etxeberria, A. Arbe, U. Gasser, A.J. Moreno, J. Colmenero, J.A. Pomposo, ACS Macro Lett. 2 (2013) 491–495.
[52] A. Arbe, J.A. Pomposo, A.J. Moreno, F. LoVerso, M. González-Burgos, I. Asenjo-Sanz, A. Iturrospe, A. Radulescu, O. Ivanova, J. Colmenero, Polym. Guildf. 105 (2016) 532–544.
[53] J.W. Chan, C.E. Hoyle, A.B. Lowe, J. Am. Chem. Soc. 131 (2009) 5751–5753.
[54] C.E. Hoyle, A.B. Lowe, C.N. Bowman, Chem. Soc. Rev. 39 (2010) 1355–1387.
[55] G.-Z. Li, R.K. Randev, A.H. Soeriyadi, G. Rees, C. Boyer, Z. Tong, T.P. Davis, C.R. Becer, D.M. Haddleton, Polym. Chem. 1 (2010) 1196–1204.
[56] D.P. Nair, M. Podgórski, S. Chatani, T. Gong, W. Xi, C.R. Fenoli, C.N. Bowman, Chem. Mater. 26 (2014) 724–744.
[57] J. Chiefari, Y.K.B. Chong, F. Ercole, J. Krstina, J. Jeffery, T.P.T. Le, R.T.A. Mayadunne, G.F. Meijs, C.L. Moad, G. Moad, et al., Macromolecules 31 (1998) 5559–5562.
[58] W.A. Braunecker, K. Matyjaszewski, Prog. Polym. Sci. 32 (2007) 93–146.
[59] R. Braslau, F. Rivera, C. Tansakul, React. Funct. Polym. 73 (2013) 624–633.
[60] M. Le Neindre, B. Magny, R. Nicolaÿ, Polym. Chem. 4 (2013) 5577–5584.
[61] C.J. Ferguson, R.J. Hughes, D. Nguyen, B.T.T. Pham, R.G. Gilbert, A.K. Serelis, C.H. Such, B.S. Hawkett, Macromolecules 38 (2005) 2191–2204.
[62] W.R. Nummy, Vinylbenzyl Thiolesters of Carboxylic Acids and Polymers Thereof US2947731, 1960.
[63] R. Nicolaÿ, Macromolecules 45 (2012) 821–827.
[64] S.N. Maiti, P. Spevak, M.P. Singh, R.G. Micetich, Synth. Commun. 18 (1988) 575–581.
[65] E. Ozden-Yenigun, E. Simsek, Y.Z. Menceloglu, C. Atilgan, Phys. Chem. Chem. Phys. 15 (2013) 17862.
[66] L.J. Fetters, N. Hadjichristidis, J.S. Lindner, J.W. Mays, J. Phys. Chem. Ref. Data 23 (1994) 619–640.
[67] J.A. Pomposo, I. Perez-Baena, F. Lo Verso, A.J. Moreno, A. Arbe, J. Colmenero, ACS Macro Lett. 3 (2014) 767–772.
[68] T.E. Dukette, M.E. Mackay, B. Van Horn, K.L. Wooley, E. Drockenmuller, M. Malkoch, C.J. Hawker, Nano Lett. 5 (2005) 1704–1709.
[69] E.B. Berda, E.J. Foster, E.W. Meijer, Macromolecules 43 (2010) 1430–1437.